PHYSICAL REVIEW B **81**, 020501(R) (2010)

Low-temperature transition to a superconducting phase in boron-doped silicon films grown on (001)-oriented silicon wafers

C. Marcenat,[1] J. Kačmarčík,[1,2] R. Piquerel,[1] P. Achatz,[1] G. Prudon,[3] C. Dubois,[3] B. Gautier,[3] J. C. Dupuy,[3] E. Bustarret,[4] L. Ortega,[4] T. Klein,[4,5] J. Boulmer,[6] T. Kociniewski,[6] and D. Débarre[6]

[1]*CEA, Institut Nanosciences et Cryogénie, SPSMS-LATEQS, 17 rue des Martyrs, 38054 Grenoble, France*

[2]*Centre of Very Low Temperature Physics, IEP Slovak Academy of Sciences and FS UPJŠ, 040 01 Košice, Slovakia*

[3]*Institut des Nanotechnologies de Lyon, CNRS and INSA, 7 av. J. Capelle, 69621 Villeurbanne, France*

[4]*Institut Néel, CNRS, BP 166, 38042 Grenoble, France*

[5]*Institut Universitaire de France and Université Joseph Fourier, BP 53, 38041 Grenoble, France*

[6]*Institut d'Electronique Fondamentale, CNRS, Université Paris Sud, 91405 Orsay, France*

(Received 28 October 2009; revised manuscript received 2 December 2009; published 4 January 2010)

We report on a detailed analysis of the superconducting properties of boron-doped silicon films grown along the 001 direction by gas immersion laser doping. The doping concentration c_B has been varied up to ~10 at. % by increasing the number of laser shots to 500. No superconductivity could be observed down to 40 mK for doping level below ~2 at. %. The critical temperature T_c then increased steeply to reach ~0.6 K for $c_B \sim 8$ at. %. No hysteresis was found for the transitions in magnetic field, which is characteristic of a type II superconductor. The corresponding upper critical field $\mu_o H_{c2}(0)$ was on the order of 1000 G, much smaller than the value previously reported by Bustarret *et al.* [E. Bustarret *et al.*, Nature (London) **444**, 465 (2006)].

DOI: 10.1103/PhysRevB.81.020501 PACS number(s): 74.62.Dh, 73.61.Cw, 74.70.Ad, 74.78.Fk

The discovery of a superconducting transition around 40 K in the MgB_2 compound[2] revived the interest for a specific class of superconducting materials: the covalent metals.[3,4] Indeed, the high T_c value is here a direct consequence of the strong coupling of the boron σ bands (shifted up to the Fermi level due to the presence of Mg^{2+} ions) with phonons. This system was the precursor of new covalent superconductors among which boron-doped diamond C:B,[5] silicon Si:B,[1] silicon carbide SiC:B,[6] as well as gallium doped germanium.[7]

Even though these systems share the similarity of being heavily doped semiconductors for which superconductivity appears in the partially unfilled valence band, they also present striking differences. In diamond, the onset of doping-induced superconductivity coincides with the metal-insulator transition (MIT).[8] On the other hand, although silicon becomes metallic for boron doping on the order of 80 ppm, a concentration of several percent was necessary to trigger superconductivity.[1] Such a concentration exceeds the solubility limit and can only be reached using sophisticated out-of-equilibrium doping techniques. This explains why a systematic study of the evolution of T_c vs boron doping in Silicon is still lacking.

We present here such a study for a series of high quality boron-doped silicon films. No superconductivity could be observed down to 40 mK for doping levels up to ~2 at. %. T_c then rises sharply with boron concentration reaching ~0.6 K for $c_B \sim 8$ at. %, a twice larger temperature than reported previously.[1] A similar rapid increase in T_c vs doping has been reported in B-doped diamond films for which T_c scales as $(c_B/c_c\text{-}1)^{0.5}$ (Ref. 8), where c_c is the critical concentration corresponding to both the MIT and the onset of superconductivity. As shown below, a similar dependence may also roughly apply to the present results but would require the use of a c_c value on the order of 2 at. %, i.e., well above the MIT doping threshold. We also show that, despite their higher T_c values, the upper critical field $H_{c2}(0)$ of our high quality films is about four times lower than the one previously reported in Ref. 1.

In order to overcome the solubility limit, a set of samples have been prepared by gas immersion laser doping (GILD).[1,9] A precursor gas (BCl_3) is chemisorbed on a (001)-oriented silicon wafer which is subsequently melted using an ultraviolet laser pulse. During each melting/solidification cycle, boron diffuses from the surface into molten silicon, and is incorporated at substitutional sites of the crystal as the liquid/solid interface moves back to the surface of the epilayer upon cooling after the laser pulse. The in-plane lattice match to the substrate and the local incorporation of boron atoms of lower covalent radius result in the formation of biaxially strained pseudomorphic epilayers. The B concentration was progressively increased by increasing the number of laser shots, from 1.4 at. % (50 shots) up to ~10 at. % (500 shots), the laser energy being regulated in order to keep the doped layer thickness constant during the whole process, here on the order of 80–90 nm. Since our previous publication,[1] new laser optics has strongly improved the spatial homogeneity in energy within the spot and an ultrahigh residual vacuum ($p \sim 10^{-7}$ Pa) is reached in the reaction chamber.

Measurements of boron concentration depth profiles were done by secondary ion mass spectrometry (SIMS) using a CAMECA IMS4f instrument. Reliable quantification of boron in silicon for such high concentration levels above 1 at. % is a major challenge for SIMS analysis due to matrix effects[10] as complex ionization and/or sputtering mechanisms may occur during secondary ion emission. We have shown that these effects remain small with an O_2^+ beam in presence of a saturated oxygen flow at the surface.[11] A primary 4 keV O_2^+ sputtering beam of 90 nA is rastered at oblique incidence (46.8°) on 250×250 μm^2 of the surface. To avoid crater edge effects, $^{10}B^+$, $^{11}B^+$, and $^{29}Si^+$ ions coming from a central part of 10 μm in diameter have been selected

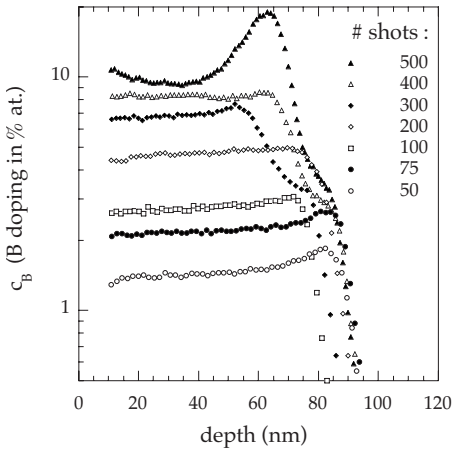

FIG. 1. Boron atomic concentration depth profiles deduced from SIMS measurements for the indicated numbers of lasers shots in the GILD process.

and analyzed simultaneously by an original isotopic comparative method (ICM) (for details see Ref. 12). Atomic concentrations are presented in Fig. 1 as a function of the depth measured by mechanical profilometry with a Tencor P10. High resolution x-ray diffraction (XRD) curves were then collected around the [004] symmetric Bragg reflection of silicon and are displayed in Fig. 2. A monochromatized Cu $K_{\alpha 1}$ excitation source led to an angular resolution better than $5 \times 10^{-3\circ}$.

Data shown in Figs. 1 and 2 illustrate the significant improvement of the structural quality and sample homogeneity with respect to previous publications.[1,9] Up to 200 shots ($c_B \leq 4.5$ at. %), we observe relatively flat boron concentrations (Fig. 1) with a sharp interface, at 80–90 nm, on the order of 9 nm/decade. The peaks in XRD (Fig. 2) remain very well-defined with a full width at half maximum on the order of 0.1°. As the number of laser shots is increased, the shift to higher diffraction angles illustrates the contraction of the out-of-plane lattice parameter $a_\perp$ as a result of the presence of boron atoms with a smaller covalent radius than silicon. This is a good indication of a sufficiently rapid recrystallization limiting the diffusion processes and leading to an homogeneous incorporation of boron on substitutional sites far above the solubility limit of 1.2 at. %. In this range, as illustrated by the inset of Fig. 2, the out-of-plane negative strain deduced from the diffraction patterns varied linearly with boron incorporation as measured by SIMS, the slope being in fair agreement with the strain rate coefficient of Vegard's law in silicon.[13] Above 200 shots, the interface began to exhibit a shoulder or even a large peak (500 shots) indicating a pileup of boron at the interface during the process. The diffraction peaks did not shift upwards anymore and remained close to 36°. Their intensity weakened and their width increased substantially, a second weaker broad peak even developing around 35.5° for 500 laser shots. This corresponds to a saturation of the out-of-plane strain around −3.5%. Since according to SIMS measurements the intake of boron went on increasing between 200 and 500 shots, one is led to conclude that in this range, an increasing fraction of these boron atoms were not incorporated on substitutional sites. In our experience, the saturation value of 36.1° observed here for the [004] diffraction peak of Si:B is a quite general upper limit, independent of our GILD operation conditions.

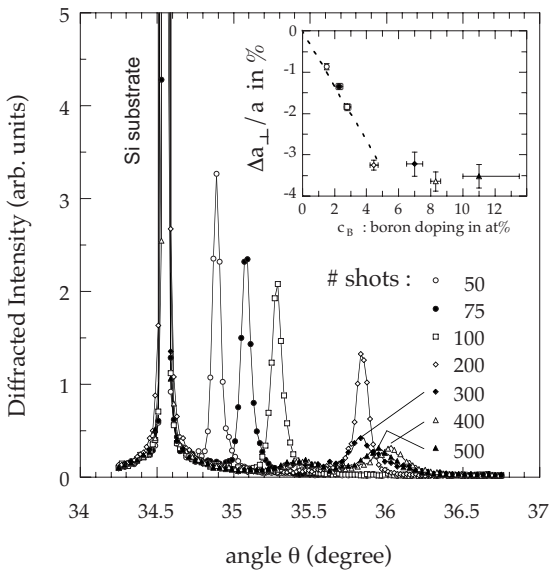

FIG. 2. High-resolution XRD measurements of Si:B films at [004] Bragg reflection. The peak at 34.565° corresponds to the Si substrate and the second peak is characteristic of the doped layer for the indicated numbers of laser shots in GILD process. Inset: relative variation in the lattice parameter perpendicular to the surface in % as a function of the boron concentration c_B. Broken line, linear dependence (Vegard's law) at low doping.

The superconducting temperatures and upper critical field have been deduced from ac-susceptibility (χ_{ac}) and magnetotransport (R) measurements. In the χ_{ac} measurements, the films have been placed on top of miniature coils, and T_c has been obtained by detecting the change in the self-induction of the coils induced by the superconducting transitions. Both ac and dc magnetic fields were applied perpendicularly to the doped layer. Approximate corrections were made to account for the demagnetization factor, but they do not affect the determination of H_{c2}, where the magnetization is zero. As shown in the inset of Fig. 3, the onset of the diamagnetic response well coincides with the resistive transition, which is remarkably sharp in this sample, $\Delta T_c \sim 10$ mK, while being only five times larger in the other samples of the series. This allows an accurate determination of T_c, and the corresponding values have been reported in Fig. 3 as a function of the B content deduced from SIMS measurements.

No superconductivity was found down to 40 mK for the two less doped samples with $c_B \sim 1.4$ at. % (50 laser shots) and $c_B \sim 2.2$ at. % (75 laser shots). For higher boron concentration, the critical temperature increases sharply with doping reaching 0.6 K for $c_B \sim 8$ at. %. For comparison, the sample measured in[1] displayed a roughly twice smaller T_c with a much broader transition. The apparent saturation of T_c is probably nonintrinsic since the incorporated boron in this range of concentration might be nonelectrically active as suggested by XRD and by the observation of a maximum angle of diffraction with broad and less intense peaks (see above). Calculations within density functional theory and

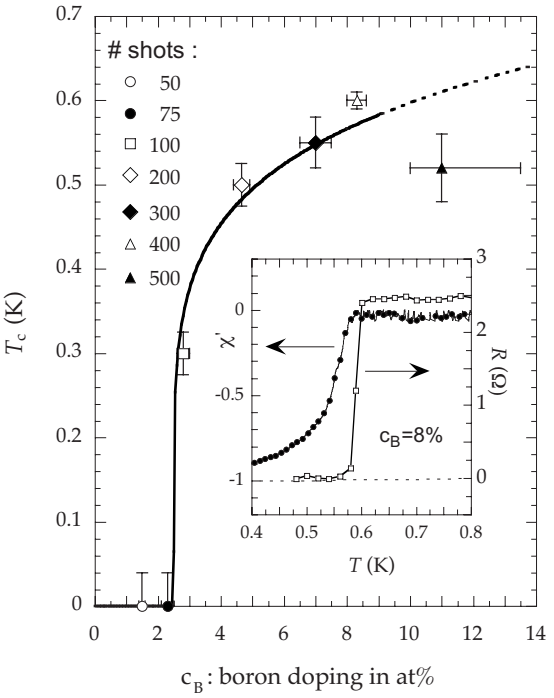

FIG. 3. Dependence of the superconducting transition temperature T_c on the boron concentration c_B deduced from SIMS measurements. In the inset: resistive (right scale) and magnetic (left scale) transition in zero magnetic field in a Si:B film (400 laser shots and $c_B \sim 8$ at. %) showing that both transport and diamagnetic transitions are very sharp and occur at the same temperature.

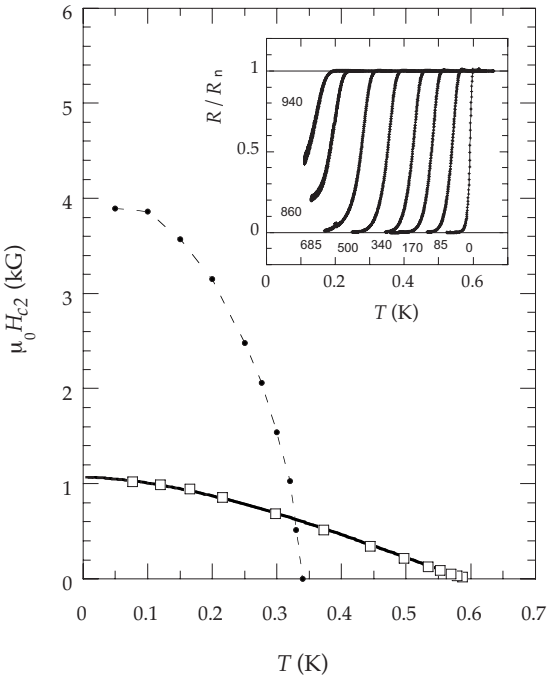

FIG. 4. Temperature dependence of the upper critical field H_{c2} deduced from transport measurements (see inset) in a heavily doped Si:B samples ($c_B \sim 8$ at. %, open squares; classical theory in the very dirty limit, full line) together with the values previously reported in Ref. 1 (dots and dashed line). In the inset: temperature dependence of the resistance normalized to its normal state value in a series of magnetic fields given in Gauss

virtual crystal approximation[14] predict $T_c \sim 0.3$ K (respectively, 3 K) for $c_B = 5$ at. % (respectively, 10 at. %) using MacMillan formula.[15] Even if the order of magnitude is correct, the observed dependence of T_c on c_B is strikingly different from these predictions. $T_c(c_B)$ is actually very similar to that observed in doped diamond, with a critical threshold for doping concentration c_c above which T_c increases very sharply with a quasipower law dependence, $T_c \propto (\frac{c_B}{c_c} - 1)^{0.5}$. Whereas in doped diamond, c_c coincides with the critical concentration of the metal-insulator transition, in doped silicon $c_c \sim 2$ at. %, i.e., about 300 times larger than the concentration necessary to induce metallicity. The meaning of c_c in this latter case remains, therefore, rather puzzling and needs to be clarified by further studies.

Electrical measurements were performed in magnetic field on the sample with $c_B \sim 8$ at. % (400 laser shots), which has the highest T_c and the sharpest transition in zero field. The results are displayed in the inset of Fig. 4 as temperature was swept at different fixed magnetic fields. The transitions were shifted toward lower temperature as the magnetic field was increased, while remaining sharp and well-defined. No hysteresis nor supercooling was observed, indicating a second-order transition, which is consistent with doped silicon being a type II superconductor. The upper critical magnetic field H_{c2}, defined by the usual criterion as where the resistance is 90% of its normal state value, is plotted in Fig. 4. Note that the discussion below and the shape of the critical line don't depend on the exact criterion used; a $R/R_n = 50\%$ definition would only shift slightly the $H_{c2}(T)$ line.

The temperature dependence of H_{c2} is very well-reproduced within the standard microscopic theory. The full line in Fig. 4 is a fit to the solution of the linearized Gor'kov equations neglecting spin effects[16] in the very dirty limit, $\frac{\ell}{\xi} \to 0$, ℓ being the electronic mean-free path and ξ the superconducting coherence length. Both the strong curvature and a four times larger $H_{c2}(T=0\ \text{K})$ observed previously[1] were most probably a consequence of the film inhomogeneity. Since the Fermi velocity v_F is a parameter that cannot be determined experimentally with any accuracy, the electronic mean-free path ℓ and $H_{c2}(0)$ were estimated in a simple two-band free electron model[17] with light (subscript *lh*) and heavy (subscript *hh*) holes having an effective mass $m^*_{lh} = 0.16\ m_e$ (respectively, $m^*_{hh} = 0.49\ m_e$), m_e being the bare electron mass, and with a total carrier concentration of 4×10^{21} cm^{-3}.

The residual resistivity in this sample was on the order of $\rho_o \sim 100\ \mu\Omega$ cm leading to $\ell = \frac{\sqrt{\langle v_F^2 \rangle}}{\rho_o e^2} (\frac{n_{lh}}{m^*_{lh}} + \frac{n_{hh}}{m^*_{hh}})^{-1} \sim 2-3$ nm. The light hole band is expected to play a minor role for the determination of the upper critical field due to its larger Fermi velocity and its lower partial density of states. In the dirty limit, H_{c2} is, therefore, related to the electronic mean-free path ℓ and to the coherence length in the heavy hole band ξ_{hh} by: $\mu_o H_{c2} \approx \frac{3\Phi_o}{2\pi^2 l \xi_{hh}}$ (Refs. 18 and 19) with ξ_{hh} being renormalized by the electron-phonon coupling constant $\lambda_{ep} \sim 0.3$ (Ref. 1) to $\xi_{hh} = \frac{\hbar v_F^{hh}}{\pi \Delta (1+\lambda_{ep})} \sim 1000$ nm, Δ being the superconducting gap. Finally, one obtains $\mu_o H_{c2}(0) \sim 1000-1200$ Gauss, which is in good agreement with

the experimental data (see Fig. 4) considering the uncertainties in the thickness of the film and in the geometry of the contacts in a van der Pauw configuration together with the crudeness of a free electron approximation. Note that the London penetration depth $\lambda_L = \sqrt{\frac{(1+\lambda_{ep})}{\mu_o e^2}\left(\frac{n_{lh}}{m^*_{lh}} + \frac{n_{hh}}{m^*_{hh}}\right)^{-1/2}}$ ~ 60 nm $\ll \xi$, implying that doped Si should be intrinsically a type I superconductor such as SiC:B (Ref. 20) but is turned into a type II system by strong impurity effects ($\kappa \sim 0.7\lambda_L/\ell \geq 1$ in the dirty limit but $\kappa = \lambda_L/\xi \leq 1$ in the clean limit).

To conclude, the GILD technique is proved to be a powerful technique to dope silicon in the alloying range where superconductivity occurs. The superconducting transitions are sharp and well-defined both in resistivity and magnetic susceptibility allowing the study of the variation in T_c on the boron concentration. This variation is in contradiction with a classical exponential dependence on superconducting parameters. Instead, T_c increases with a quasipower law form above a critical threshold c_c in striking similarity to what is observed in doped diamond. Although in the diamond case c_c was equal to the MIT critical concentration, in silicon, it lies far above. The comparison of these two cases offers a playground for studying superconductivity in covalent systems near a MIT.

[1] E. Bustarret *et al.*, Nature (London) **444**, 465 (2006).
[2] J. Nagamatsu, N. Nakagawa, T. Muranaka, Y. Zenitani, and J. Akimitsu, Nature (London) **410**, 63 (2001).
[3] X. Blase, E. Bustarret, T. Klein, C. Chapelier, and C. Marcenat, Nature Mater. **8**, 375 (2009).
[4] V. H. Crespi, Nature Mater. **2**, 650 (2003).
[5] E. A. Ekimov *et al.*, Nature (London) **428**, 542 (2004).
[6] Z.-A. Ren, J. Kato, T. Muranaka, J. Akimitsu, M. Kriener, and Y. Maeno, J. Phys. Soc. Jpn. **76**, 103710 (2007).
[7] T. Herrmannsdorfer *et al.*, Phys. Rev. Lett. **102**, 217003 (2009).
[8] E. Bustarret, J. Kačmarčik, C. Marcenat, E. Gheeraert, C. Cytermann, J. Marcus, and T. Klein, Phys. Rev. Lett. **93**, 237005 (2004); T. Klein *et al.*, Phys. Rev. B **75**, 165313 (2007).
[9] G. Kerrien *et al.*, Appl. Surf. Sci. **208-209**, 277 (2003).
[10] A. Benninghoven, F. Rüdenauer, and H. Werner, *Secondary Ion Mass Spectrometry: Basics Concepts, Instrumental Aspects, Applications and Trends* (WiIey, New York, 1987), Chap. 3, p. 281.
[11] C. Dubois *et al.*, in Proceedings of International Conference on Secondary Ion Mass Spectrometry (SIMS XVII), Toronto, September 2009, edited by J. Gardella (unpublished).
[12] C. Dubois, G. Prudon, B. Gautier, and J. C. Dupuy, Appl. Surf. Sci. **255**, 1377 (2008).
[13] A. Vailionis, G. Glass, P. Desjardins, D. G. Cahill, and J. E. Greene, Phys. Rev. Lett. **82**, 4464 (1999).
[14] L. Boeri, J. Kortus, and O. K. Andersen, Phys. Rev. Lett. **93**, 237002 (2004).
[15] J. P. Carbotte, Rev. Mod. Phys. **62**, 1027 (1990).
[16] E. Helfand and N. R. Werthamer, Phys. Rev. **147**, 288 (1966).
[17] A similar analysis was made in the superconductor $MgCNi_3$ in A. Wälte, G. Fuchs, K.-H. Müller, A. Handstein, K. Nenkov, V. N. Narozhnyi, S. L. Drechsler, S. Shulga, L. Schultz, and H. Rosner, Phys. Rev. B **70**, 174503 (2004).
[18] P. G. de Gennes *et al.*, Phys. Kondens. Mater. **3**, 79 (1964).
[19] K. Maki, Physics (N.Y.) **1**, 21 (1964).
[20] M. Kriener, Y. Maeno, T. Oguchi, Z. A. Ren, J. Kato, T. Muranaka, and J. Akimitsu, Phys. Rev. B **78**, 024517 (2008).